Journal of ELECTRONIC MATERIALS, Vol. 45, No. 9, 2016
DOI: 10.1007/s11664-016-4729-5

Band Offsets of III–V and II–VI Materials Studied by Temperature-Dependent Internal Photoemission Spectroscopy

A.G.U. PERERA,[1,4] Y.F. LAO,[1] P.S. WIJEWARNASURIYA,[2] and S.S. KRISHNA[3]

1.—Department of Physics and Astronomy, Georgia State University, Atlanta, GA 30303, USA. 2.—U.S. Army Research Laboratory, Adelphi, MD 20783, USA. 3.—Center for High Technology Materials, Department of Electrical and Computer Engineering, University of New Mexico, Albuquerque, NM 87106, USA. 4.—e-mail: uperera@gsu.edu

The band offset at the interface of a heterojunction is one of the most important parameters determining the characteristics of devices constructed from heterojunction. Accurate knowledge of band offsets and their temperature dependence will allow one to simulate and predict the device performances. We present a temperature-dependent internal-photoemission spectroscopy (TDIPS) for studying the band offsets. Applications of the TDIPS into III–V and II–VI materials are discussed.

Key words: Heterojunction, internal photoemission, III-V, II-VI

INTRODUCTION

Internal photoemission (IPE) spectroscopy has been extensively used[1–3] to study the band parameters of materials at the interface of two materials. The IPE process can be characterized by the quantum yield, defined as the number of emitted carriers per one absorbed photon. The theoretical basis of IPE was on the basis of the Fowler's work[4] on external photoemission of electrons from metal to vacuum. The photoemission yield function deduced by Fowler has the following form, expressed by

$$Y \sim (kT)^2 \cdot f(\mu) \tag{1}$$

which includes temperature-dependent (T-dependent) terms. Y denotes the quantum yield, which can be obtained in experiment as the multiplication of spectral responsivity and photon energy. $f(\mu)$ is defined as,[4]

$$f(\mu) = \begin{cases} e^{\mu} - e^{2\mu}/4 + \cdots & (\mu 0) \\ \pi^2/6 + \mu^2/2 - (e^{-\mu} - e^{-2\mu}/4 + \cdots) & (\mu 0) \end{cases} \tag{2}$$

(Received September 22, 2015; accepted June 3, 2016; published online June 22, 2016)

where

$$\mu = (h\nu - \Delta)/kT \tag{3}$$

$h\nu$ is the photon energy. When $h\nu$ is greater than $\Delta + 3kT$,[5] the Fowler's yield function can be simplified and reduced to a form without containing T-dependent terms f, i.e.,

$$Y \sim (h\nu - \Delta)^2 \tag{4}$$

Although Fowler's yield function was derived to be used in external photoemission studies, it has been applied[6] to IPE processes as well. To adapt to the difference of the carrier transit in semiconductors from the metal, the exponent "2" in Eq. 4 was replaced by a different constant p,[7–10] typically varying from 1 to 3.[10] Despite that a best-fit of p can be achieved in order to fit experimental yield, its meaning is unclear. In addition, the lack of taking the T-dependence into account leads to underestimation of the Δ values. Such a consequence could cause significant divergence in semiconductor structures which have the value of Δ much < 1 eV.

In contrast to Fowler's yield formalism, the temperature-dependent internal-photoemission spectroscopy (TDIPS) discussed here takes into account the carrier thermalization and carrier/dopant-induced band-renormalization and band-tailing effects, and thus measures the band offset at different temperatures.

THE PRINCIPLE OF TDIPS

The principle of TDIPS is depicted in Fig. 1, in which the inset shows the transfers of carriers from the valence bands of the emitter to those of the barrier. For the holes with energies near the barrier band edge and escaping over the barrier, they contribute to yield spectrum around the threshold. In this case, the indirect transitions have the dominant contributions. With increase of the photon energy much greater than the threshold, high-energetic holes excited through direct transitions are capable of escaping over the barrier and contributing to the yield.

In the case of determining the band offsets, the primary processes including an energy distribution function of the holes $\rho(\epsilon, h\nu - E_f)$ through inter-valence-band (IVB) transitions[11] and a probability function describing their transmission over the barrier $P(\epsilon, \Delta)$ are taken into account, leading to the following expression of the quantum yield,

$$Y(h\nu) = Y_0(kT) + C_0 \int_{\Delta}^{\infty} P(\epsilon, \Delta) \cdot \rho(\epsilon, h\nu - E_f) f(\epsilon, h\nu)\, d\epsilon \tag{5}$$

where $Y_0(kT)$ is a thermionic emission term, C_0 is a constant independent of ϵ and $h\nu$, ϵ is the energy of photoexcited holes, and Δ is defined as the energy difference between the Fermi level and the valence band edge of the barrier. $f(\epsilon, h\nu)$ takes the form of $\left[1 + e^{(\epsilon - h\nu)/kT}\right]^{-1}$, in analogy to the Fermi–Dirac (FD) statistics. The use of the FD-like function is based on an assumption that photoexcited holes remain the same distribution as that before photoexcitation. The difference between the distribution before and after photoexcitation is an energy of $h\nu$.

The photoexcitation of holes in the absorber and their escape over the barrier has the predominant contribution to the quantum yield. In contrast, the spectral line shape of the quantum yield is primarily determined by the energy distribution of photoexcited holes, which can approximate to $\rho(\epsilon, \epsilon_0) \sim (\epsilon - \epsilon_0)^{1/2}$.[1] Due to the heavy doping in emitters, $\rho(\epsilon, \epsilon_0)$ must take into account dopant-related effects, for example, the band tail. A Kane model[12] was applied to obtain a band tailing.

It is expected that the carrier-phonon scattering comes into play at the above-threshold regime, where the excess kinetic energy of carriers is greater than the phonon energy. After scatterings, a portion of photocarriers will have less energy than the barrier, and thus be incapable of a successful escape. This should lead to degradation in the photoresponse. We have recently demonstrated the IPE approach in studying the scattering effects[13] by fitting of the near-threshold quantum yield spectra.

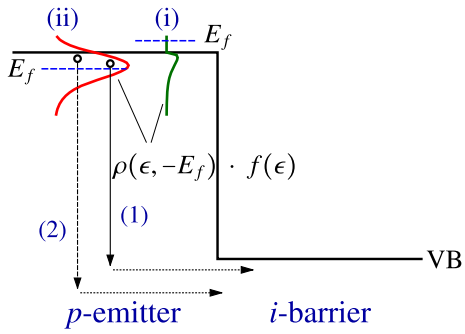

Fig. 1. The valence band diagram of a heterojunction consisting of a p-emitter and an i-barrier. $\rho(\epsilon, -E_f) f(\epsilon)$ denotes the multiplication of the hole energy distribution (ρ) and the FD function (f). (i) and (ii) correspond to non-degenerate and degenerate doped emitters, respectively. The IPE processes are labeled as (1) and (2), owing to optical transitions in the emitter and then escaping over the barrier.

TDIPS ANALYSIS OF p-TYPE GAAS/ $AL_xGA_{1-x}AS$ HETEROJUNCTIONS

The quantum yield spectra of GaAs/Al_xGa_{1-x}As heterojunctions (as shown in Table I) were analyzed to obtain their VB offsets. Figure 2(a–d) shows the fittings. The values of Δ are extrapolated at zero bias voltage in order to avoid the calculation of image-force barrier lowering $\Delta\phi_i$. The VB offsets were obtained using $\Delta E_v = \Delta - \Delta_{\mathrm{BGR}} + E_f + \Delta\phi_i$. Results indicate a T-dependent ΔE_v as a function of Al mole fraction for GaAs/Al_xGa_{1-x}As, i.e., $\Delta E_v = (0.570 - 1.39 \times 10^{-4} \cdot T)\, x$ (eV). This also means that, the band offset ratio r (defined as $\Delta E_c : \Delta E_v$) varies from 59 : 41 at 4.2 K[14] to 61 : 39 at 300 K for $x = 0.4$; the latter is nearly the same as the suggested value 62 : 38 by Kroemer.[15]

TDIPS ANALYSIS OF PHOTODETECTORS WITH WAVELENGTH EXTENSION

TDIPS[1] was used to analyze photodetectors with wavelength extension, as shown in Fig. 3. The TDIPS fitting results are compared with experimental yield spectra in the near-threshold regime. Fig. 3b shows the fitted threshold energies at different biases, along with a comparison with the activation energy as a function of bias obtained from Arrhenius plots. It is noted that for the value of the negative bias greater than 0.6 V, good agreement with experiment (Fig. 3) can be achieved by modelling the system using two photoemission processes, leading to two threshold energies (as illustrated in the inset of Fig. 3). The thresholds with low-energy values agree with those obtained by the one-threshold TDIPS fittings. They originate from the wavelength extended response. In contrast, the high-energy thresholds are associated with the "normal" response where the threshold is determined by Δ.

According to Arrhenius plots, the activation energy at 0 V is 0.40 eV (or 3.1 μm in wavelength), corresponding to the barrier height of the p-type GaAs/$Al_{0.75}Ga_{0.25}$As junction. However, TDIPS

Table I. GaAs/$Al_xGa_{1-x}As$ heterojunction detectors, consisting of the same emitter thickness of 18.8 nm

Sample number	Al mole fraction, x	Barrier thickness (nm)	Emitter doping (cm^{-3})	Periodicity
S12a	0.12	125	1×10^{17}	16
S12b	0.12	125	1×10^{18}	16
S15	0.15	125	3×10^{18}	12
S28	0.28	60	3×10^{18}	30
S37	0.37	60	3×10^{18}	30
S57	0.57	60	3×10^{18}	30

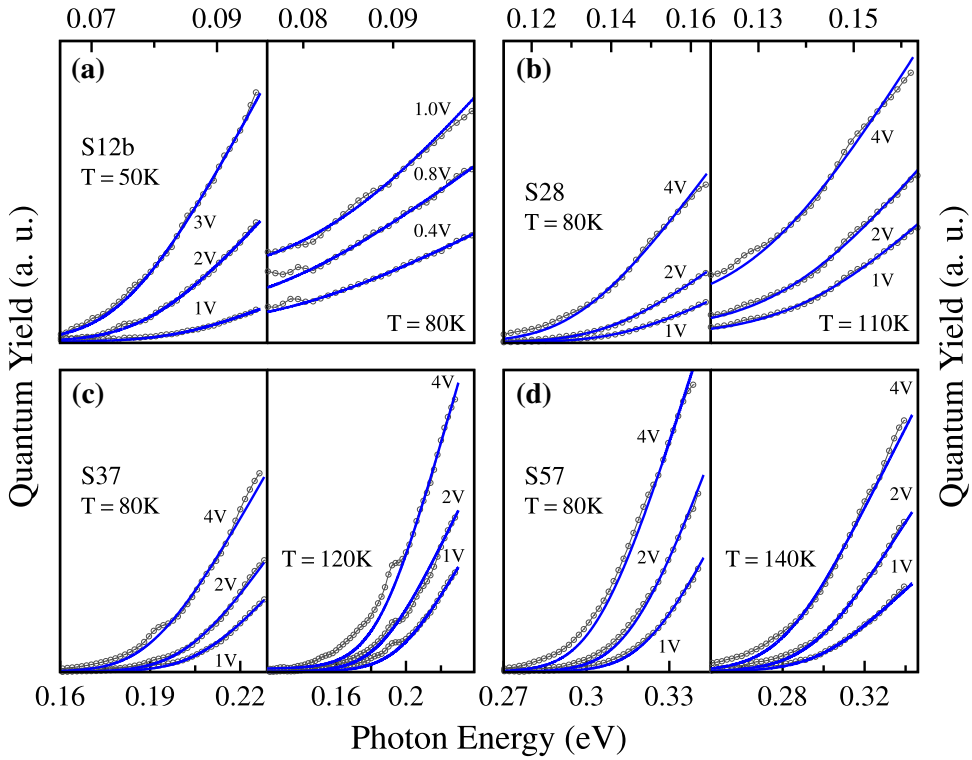

Fig. 2. (a)–(d) are experimental (scattered data) quantum yield spectra of GaAs/$Al_xGa_{1-x}As$ heterojunctions (see Table 1 for structures). The TDIPS fittings based on Eq. 5 with Y_0, C_0 and Δ as the fitting parameters are shown as *solid lines*. The thermionic emission yield (Y_0) increases with biases and temperature.

fittings to measured spectral response gives a threshold energy of 0.14 eV (8.9 μm in wavelength) nearly independent of bias, which indicates a wavelength extension from 3.1 μm to 8.9 μm.

TDIPS ANALYSIS OF TYPE-II STRAINED LAYER SUPERLATTICE DETECTORS

TDIPS has also been demonstrated to understand the operation of a pBp T2SL detector. Figure 4a shows its structure, consisting of two *p*-type InAs/GaSb T2SL absorbers that are responsible for the mid/long-wave infrared (MWIR/LWIR) absorption. These two absorbers are separated by a barrier (B)-region (InAs/AlSb T2SL). The motivation of this study is to obtain the conduction band offset that affects the transport of minority electrons.

Optical transitions take place across the band gap of the absorbers (I), the band gap of the B-region (II), and the valence band offset between the absorber and the B-region interface (III). All of these can be observed on the quantum yield (Y) spectra as plotted in Fig. 4b, where fittings to quantum yield spectra in different near-threshold energy regimes were also carried out. This leads to the band gaps of the LWIR and MWIR absorbers determined to be 0.117 ± 0.002 eV and 0.157 ± 0.001 eV, respectively, in a good agreement with the nominal values of 0.103 eV and 0.159 eV.[16] TDIPS fitting also determines a VB offset of 0.661 ($\pm$0.002) eV. Based on these parameters, the conduction band offset at the interface between the LWIR absorber and the B-region is obtained as 0.004 ± 0.004 eV, which can barely affect the transport of minority electrons.

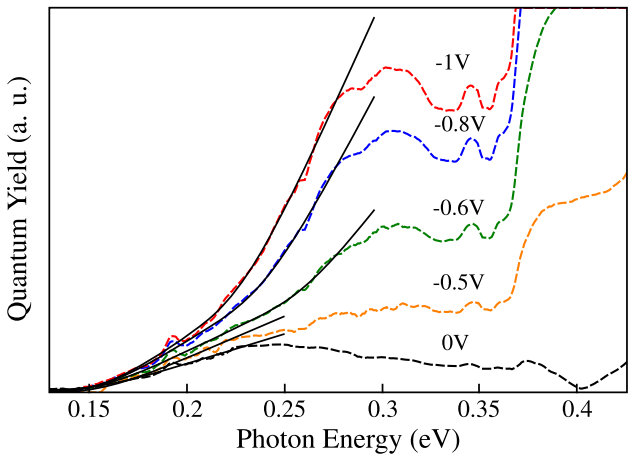

Fig. 3. Quantum yield spectra of photodetectors with wavelength extension, along with TDIPS fittings (solid lines). TDIPS fittings to measured spectral response give a threshold energy of 0.14 eV (8.9 μm in wavelength).[1]

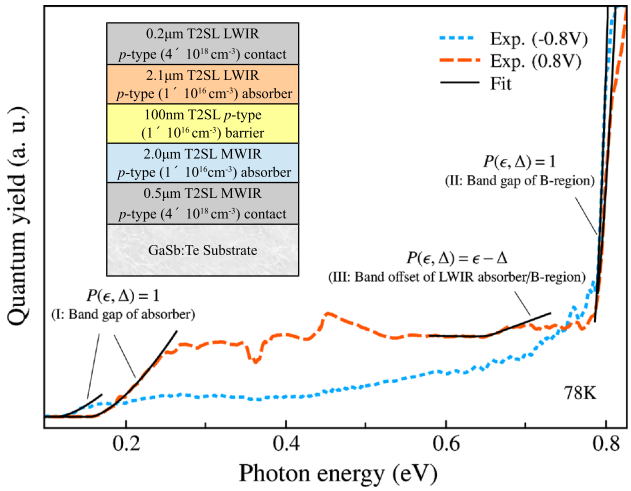

Fig. 4. Experimental quantum yield spectra of a pBp type-II InAs/GaSb superlattice detector (inset) and TDIPS fittings (based on Eq. 5). I – III represent the three optical transitions with the threshold energies fitted by TDIPS.

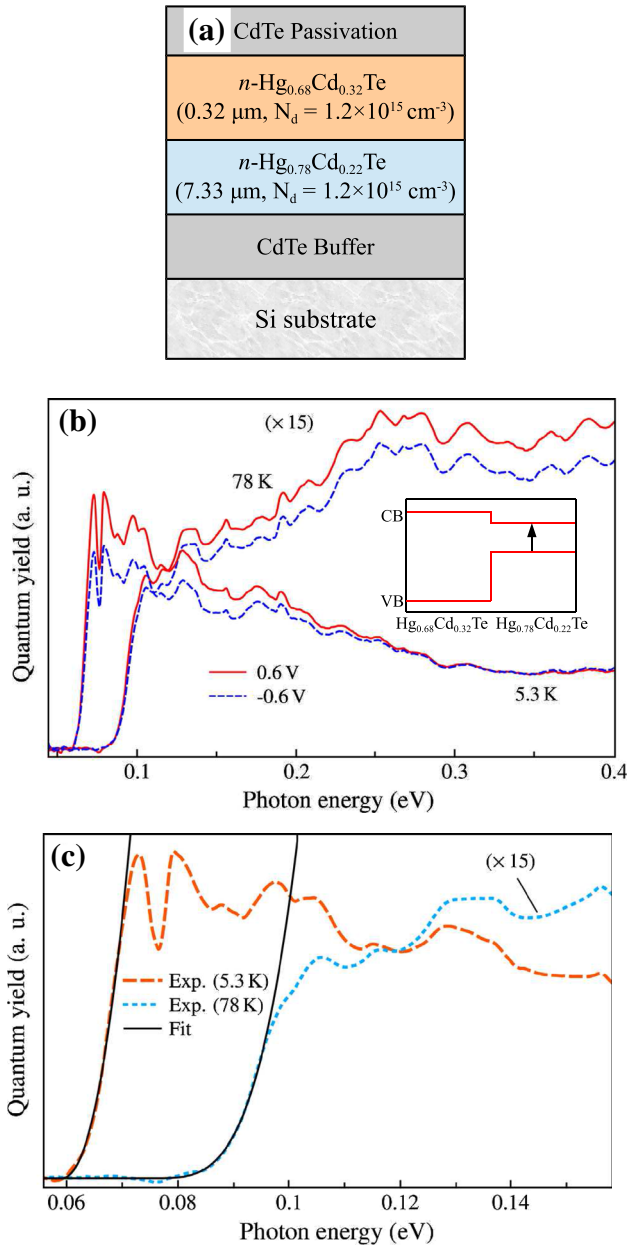

Fig. 5. (a) Structure of the *n*-type $Hg_{0.78}Cd_{0.22}Te/Hg_{0.68}Cd_{0.32}Te$ detector. (b) The quantum yield spectra measured at 5.3 and 78 K. The spectral profile under the positive bias is nearly similar to that under the negative bias at the same temperature. The inset plots the schematic band alignment (without considering the space charge effect and composition grading at the junction interface) and the dominant optical transition which occurs in $Hg_{0.78}Cd_{0.22}Te$. (c) The quantum yield spectra at 0.6 V and TDIPS fittings (solid line).

TDIPS ANALYSIS OF MCT DETECTORS

The application of the TDIPS method to study a *n*-type HgCdTe (MCT) heterojunction (Fig. 5a)[17] is described. Figure 5b shows the typical quantum yield spectra at 5.3 and 78 K. The undulation is related to the optical interference inside the substrate. The low-energy cut-off is due to the escape of photo-carriers from the absorber (originating from the optical transition schematically shown in the inset). In contrast to the trivial band tailings in GaAs materials, the Urbach tail[18] is known to distort the absorption edge of HgCdTe. For this study, the energy distribution (ρ) is taken to be proportional to JDOS: $JDOS \sim \alpha \times h\nu$, where $\alpha(h\nu)$ is the absorption coefficient. TDIPS fittings confirm an exponential line-shape of the absorption tail, as shown in Fig. 5c. According to the device structure, electrons escaping into the $Hg_{0.68}Cd_{0.32}Te$ layer under a positive bias need to overcome a barrier associated with the conduction band offset of the junction. However, differences in the TDIPS thresholds for positive and negative biases cannot be identified from the spectral yield plotted in Fig. 5b.

This indicates negligible electron barrier at the interface.

Previous studies assume the parabolic-band approximation (PBA), i.e., $JDOS \sim (\epsilon - hv)^{1/2}$, for GaAs/AlGaAs heterojunctions[1] and type-II InAs/GaSb superlattice structures,[13] where dopant-caused band tailing effects are neglected. However, the Urbach tail[18] can significantly distort the absorption edge of HgCdTe. The IPE fittings based on PBA show good agreement with the experimental spectra at the high-energy range. However, there is a mismatch between the fitting and experiment in the near-threshold regime, as shown in the inset of Fig. 5c. For this reason, band tailing should be taken into account in order to fit the yield spectra (see the inset of Fig. 5c).

Based on Fig. 5b, electrons have to overcome a potential barrier associated with the conduction band offset of the $Hg_{0.78}Cd_{0.22}Te/Hg_{0.68}Cd_{0.32}Te$ junction under a positive bias in order to escape; in contrast, electrons overcoming the potential barrier (under negative bias) is not needed. However, this difference was not observed on the experimental yield spectra, as shown in Fig. 5b, in which the spectra under positive and negative bias polarity display similar profile, and no apparent shifting in the thresholds was identified.

The threshold energies at positive biases should correlate with the transitions across a band gap. The minimum photon energy absorbed is thus $E_g + \Delta E_c$, where E_g is the band-gap of $Hg_{0.78}Cd_{0.22}Te$, and ΔE_c is the value of conduction band offset, in order to successfully escape over the $Hg_{0.68}Cd_{0.32}Te$ barrier. Adachi[19] suggests $\Delta E_c(x) = 1.21 - 1.21x$ for $Hg_{1-x}Cd_xTe/CdTe$. This means that the conduction band offset of $Hg_{1-x}Cd_xTe/Hg_{1-y}Cd_yTe$ is $\Delta E_c = \Delta E_c(x) - \Delta E_c(y)$, and the expected ΔE_c amounts to 0.121 eV. The threshold energy of electrons overcoming a potential barrier is subject to bias-caused lowering effect due to the image force effect.[1] However, this result was not observed in the present study. Instead, the obtained threshold agrees with the band gap of $Hg_{0.78}Cd_{0.22}Te$, in accordance with the band-gap formalism of Laurenti et al.[20] This leads to a conclusion that no potential barrier is present at the heterojunction. One of the reasons is that the band spike associated with the band offset can be smoothed out due to the composition grading at the interface. The height of the conduction barrier is determined by the width of the interfacial gradient region. From the growth point of view, the interface can be controlled, for example, by intentionally growing an interfacial composition grading layer. This may benefit a higher collection efficiency of photo-electrons owing to reduced barrier height.

CONCLUSION

In summary, a temperature-dependent internal-photoemission spectroscopy has been discussed and applied to studying the band offset at the interface of the heterojunction. TDIPS characterizations of III–V valence band offset, the band offset of type-II superlattice structures and the conduction band offset of MCT detectors are discussed.

ACKNOWLEDGEMENTS

This work was supported in part by the U.S. Army Research Office under Grant No. W911NF-12-2-0035 monitored by Dr. William W. Clark.

REFERENCES

1. Y.F. Lao, and A.G.U. Perera, *Phys. Rev. B* 86, 195315 (2012).
2. R. Yan, Q. Zhang, W. Li, I. Calizo, T. Shen, C.A. Richter, A.R. Hight-Walker, X. Liang, A. Seabaugh, D. Jena, H.G. Xing, D.J. Gundlach, and N.V. Nguyen, *Appl. Phys. Lett.* 101 (2), 022105 (2012).
3. Y. Hikita, M. Kawamura, C. Bell, and H.Y. Hwang, *Appl. Phys. Lett.* 98 (19), 192103 (2011).
4. R.H. Fowler, *Phys. Rev.* 38 (1), 45 (1931).
5. S.M. Sze, and K.K. Ng, *Physics of Semiconductor Devices* (Wiley, New York, 2007), pp. 176–178.
6. C. Coluzza, E. Tuncel, J.L. Staehli, P.A. Baudat, G. Margaritondo, J.T. McKinley, A. Ueda, A.V. Barnes, R.G. Albridge, N.H. Tolk, D. Martin, F. Morier-Genoud, C. Dupuy, A. Rudra, and M. Ilegems, *Phys. Rev. B.* 46 (19), 12834 (1992).
7. C. Caroli, J.S. Helman, and F.S. Sinencio, *Phys. Rev.* B 11, 980 (1975).
8. E.O. Kane, *Phys. Rev.* 127 (1), 131 (1962).
9. W. Seidel, O. Krebs, P. Voisin, J.C. Harmand, F. Aristone, and J.F. Palmier, *Phys. Rev. B* 55, 2274 (1997).
10. V.V. Afanas'ev and A. Stesmans, *J. Cryst. Growth* 102 (8), 081301 (2007).
11. Y.F. Lao, P.K.D.D.P. Pitigala, A.G.U. Perera, H.C. Liu, M. Buchanan, Z.R. Wasilewski, K.K. Choi, and P. Wijewarnasuriya. *Appl. Phys. Lett.* 97 (9), 091104 (2010).
12. E.O. Kane, *Phys. Rev.* 131, 79 (1963).
13. Y.F. Lao, P.K.D.D.P. Pitigala, A.G. Unil Perera, E. Plis, S.S. Krishna, and P.S. Wijewarnasuriya. *Appl. Phys. Lett.* 103 (18), 181110 (2013).
14. W. Yi, V. Narayanamurti, H. Lu, M.A. Scarpulla, and A.C. Gossard, *Phys. Rev. B* 81 (23), 235325 (2010).
15. H. Kroemer, *Rev. Mod. Phys.* 73, 783 (2001).
16. E. Plis, S. Krishna, N. Gautam, S. Myers, and S. Krishna, *Photonics J. IEEE* 3 (2), 234 (2011).
17. Y.F. Lao, A.G. Unil Perera, and P.S. Wijewarnasuriya, *Appl. Phys. Lett.* 104 (13), 131106 (2014).
18. F. Urbach, *Phys. Rev.* 92, 1324 (1953).
19. S. Adachi, P. Capper, S. Kasap, and A. Willoughby, *Properties of Semiconductor Alloys: Group-IV, III-V and II-VI Semiconductors*. Wiley Series in Materials for Electronic & Optoelectronic Applications (Burlington, MA: Academic Press, 2009).
20. J.P. Laurenti, J. Camassel, A. Bouhemadou, B. Toulouse, R. Legros, and A. Lusson, *J. Appl. Phys.* 67 (10), 6454 (1990).